Transition Metal Complexes of Optically Active Tris(pyrazolyl)hydroborates

Daniel D. LeCloux, Michael C. Keyes, Masahisa Osawa, Veronica Reynolds, and William B. Tolman*

Department of Chemistry, University of Minnesota, 207 Pleasant Street S.E., Minneapolis, Minnesota 55455

Received July 28, 1994[⊗]

The synthesis and characterization of a series of complexes of the recently reported (LeCloux, D. D.; Tokar, C. J.; Osawa, M.; Houser, R. P.; Keyes, M. C.; Tolman, W. B. *Organometallics* **1994**, *13*, 2855−2866) ligands tris(7(*R*)-isopropyl-4(*R*)-methyl-4,5,6,7-tetrahydroindazolyl)hydroborate (Tp^{Menth}) and tris(7(*S*)-*tert*-butyl-4(*R*)-methyl-4,5,6,7-tetrahydroindazolyl)hydroborate ($Tp^{Mementh}$) are presented. Specific complexes prepared are $Tp^{Menth}M^{II}Cl$ (M^{II} = Zn^{II}, Ni^{II}, Co^{II}, Cu^{II}, Mn^{II}, Fe^{II}), $Tp^{Mementh}Zn^{II}Cl$, $Tp^{Menth}M^{II}(NO_3)$ (M^{II} = Cu^{II}, Ni^{II}), $Tp^{Menth}M^{II}(OAc)$ (M^{II} = Cu^{II}, Ni^{II}), $Tp^{Menth}Rh^{I}(CO)_2$, $Tp^{Menth}Ti^{IV}Cl_3$, and $Tp^{Menth}*Ti^{IV}Cl_3$, where $Tp^{Menth}*$ is an isomerized version of Tp^{Menth} in which one pyrazolyl group is attached to boron via the more, rather than the less, hindered N atom. Structural hypotheses are proposed on the basis of analytical and spectroscopic data for all compounds and X-ray crystal structures for $Tp^{Menth}ZnCl$, $Tp^{Mementh}ZnCl$, $Tp^{Menth}Ni(OAc)$, and $Tp^{Menth}*TiCl_3$. Pseudooctahedral 4-coordinate ($Tp^{Menth}MCl$ and $Tp^{Mementh}ZnCl$), distorted square pyramidal 5-coordinate [$Tp^{Menth}M(OAc)$ and $Tp^{Menth}M(NO_3)$], and octahedral 6-coordinate ($Tp^{Menth}TiCl_3$ and $Tp^{Menth}*TiCl_3$) metal ion geometries were identified. IR and NMR data indicated that $Tp^{Menth}Rh(CO)_2$ exists as a mixture of 4- and 5-coordinate isomers. The combined synthetic, spectroscopic, and structural data for the complexes we have synthesized suggest that the chiral Tp ligands have effective steric properties similar to those of achiral variants with 3-*tert*-butyl or 3-isopropyl substituents on the pyrazolyl rings. X-ray data for $Tp^{Menth}ZnCl$: orthorhombic, space group $P2_12_12_1$ (No. 19), at −101 °C, a = 9.658(7) Å, b = 17.777(7) Å, c = 20.058(6) Å, V = 3444(5) Å^3, Z = 4, R = 0.063 and R_w = 0.049 for 4055 reflections with $I > 2\sigma(I)$ and 379 parameters. X-ray data for $Tp^{Mementh}ZnCl$: orthorhombic, space group $P2_12_12_1$ (No. 19), at 24 °C, a = 11.170(4) Å, b = 14.829(9) Å, c = 23.063(9) Å, V = 3820(5) Å^3, Z = 4, R = 0.055 and R_w = 0.056 for 4566 reflections with $I > 2\sigma(I)$ and 407 parameters. X-ray data for $Tp^{Menth}Ni(OAc)$: orthorhombic space group $P2_12_12_1$ (No. 19), at 24 °C, a = 10.139(5) Å, b = 18.248(8) Å, c = 19.700(8) Å, V = 3645(5) Å^3, Z = 4, R = 0.043 and R_w = 0.039 for 3721 reflections with $I > 2\sigma(I)$ and 406 parameters. X-ray data for $Tp^{Menth}*TiCl_3{\cdot}CH_2Cl_2$: orthorhombic, space group $P2_12_12_1$ (No. 19), at −100 °C, a = 10.335(8) Å, b = 15.430(7) Å, c = 25.11(1) Å, V = 4004(7) Å^3, Z = 4, R = 0.070 and R_w = 0.071 for 3831 reflections with $I > 2\sigma(I)$ and 424 parameters.

The well-established ability of tris(pyrazolyl)hydroborate (Tp) ligands to strongly bind metal ions,[1−4] combined with the pronounced steric effects of substituents at the 3-position of the pyrazolyl rings on the properties of the resulting metal complexes,[2] has led us to target novel optically active variants of generalized structure **A** (see Chart 1) for synthetic studies.[5,6] The C_3-symmetric array of stereogenic centers in **A** is designed to afford an unusual chiral "fence" about a coordinated metal ion that may induce interesting and potentially useful stereoselective metal-mediated reactivity.[7] We recently reported the synthesis and structural characterization of the Tl^I complexes of Tp^{Menth} and $Tp^{Mementh}$, specific examples of ligands **A** that have the particular advantages of being accessible from readily available precursors and of having stereogenic centers of fixed orientation resulting from their incorporation into fused ring systems.[6] Here we present the results of studies of the complexation behavior of these ligands with transition metal ions that demonstrate their versatile metal-binding properties and their high degree of steric bulk, akin to that documented for achiral Tp ligands with 3-*tert*-butyl or 3-isopropyl substituents.

Experimental Section

Materials and Methods. All air-sensitive reactions were performed either in a Vacuum Atmospheres glovebox under a N_2 atmosphere or by using standard Schlenk and vacuum-line techniques. The syntheses of $TlTp^{Menth}$ and $TlTp^{mementh}$, as well as general procedures used for the synthesis and characterization of new compounds, have been described.[6,8] Most of the characterization data for the complexes are listed in Table 1.

Syntheses. $Tp^{Menth}M^{II}Cl$ (M^{II} = Zn^{II}, Ni^{II}, Co^{II}, Cu^{II}). The complexes were prepared by metathesis of the Tl complex of the ligand with an excess of the metal(II) halide followed by extraction, filtration, and recrystallization. The procedure for the synthesis of $Tp^{Menth}CoCl$ is typical: A solution of $CoCl_2{\cdot}6H_2O$ (0.083 g, 0.35 mmol) in MeOH (2 mL) was added via cannula to a solution of $TlTp^{Menth}$ (0.050 g, 0.07 mmol) in CH_2Cl_2 (3 mL). After the mixture was stirred for 5 min, solvent was removed under reduced pressure, the resulting solid residue

* To whom correspondence should be addressed. FAX: 612-624-7029. E-mail: tolman@chemsun.chem.umn.edu.

⊗ Abstract published in *Advance ACS Abstracts,* November 15, 1994.

(1) Trofimenko, S. *Prog. Inorg. Chem.* **1986**, *34*, 115−210.
(2) Trofimenko, S. *Chem. Rev.* **1993**, *93*, 943−980.
(3) Shaver, A. In *Comprehensive Coordination Chemistry*; Wilkinson, G., Gillard, R. D., McCleverty, J. A., Eds.; Pergamon Press: Oxford, U.K., 1987; Vol. 2, pp 245−259.
(4) Niedenzu, K.; Trofimenko, S. *Top. Curr. Chem.* **1986**, *131*, 1−37.
(5) LeCloux, D. D.; Tolman, W. B. *J. Am. Chem. Soc.* **1993**, *115*, 1153−1154.
(6) LeCloux, D. D.; Tokar, C. J.; Osawa, M.; Houser, R. P.; Keyes, M. C.; Tolman, W. B. *Organometallics* **1994**, *13*, 2855−2866.
(7) For other examples of complexes of C_3-symmetric chiral ligands see footnote 3 in ref 6 and: Nugent, W. A.; Harlow, R. L. *J. Am. Chem. Soc.* **1994**, *116*, 6142−6148.
(8) Ruggiero, C. E.; Carrier, S. M.; Antholine, W. E.; Whittaker, J. W.; Cramer, C. J.; Tolman, W. B. *J. Am. Chem. Soc.* **1993**, *115*, 11285−11298.

0020-1669/94/1333-6361$04.50/0

Chart 1

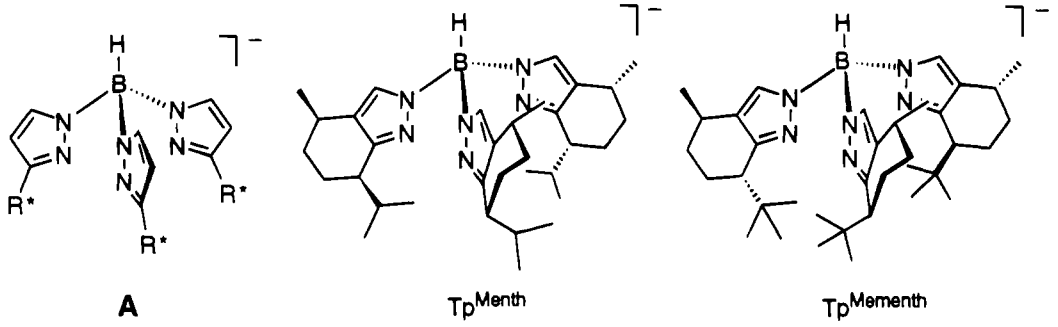

Table 1. Summary of Characterization Data

compound	α_D,[a] deg	UV−vis (nm) (ϵ (M^{-1} cm^{-1}))[b]	IR (ν_{BH})[c]	MS (*m/z*) (rel intens)[d]	elemental anal.,[e] % C	H	N
$Tp^{Menth}ZnCl$	+208 ± 4 (1.1×10^{-3})	276 (100, sh)	2470	642 (M^+, 26), 135 (100)	61.82 (61.50)	8.16 (8.13)	12.96 (13.04)
$Tp^{Mementh}ZnCl$	−460 ± 6 (9.7×10^{-4})	266 (480, sh)	2470	686 (M^+, 37), 483 (100)[f]	62.86 (62.98)	8.50 (8.52)	12.28 (12.24)
$Tp^{Menth}NiCl$	+225 ± 4 (1.0×10^{-3})	266 (3600, sh), 322 (700), 366 (150, sh), 486 (300), 806 (80)	2470	636 (M^+, 20), 600 (100)	62.39 (62.14)	8.16 (8.22)	13.39 (13.18)
$Tp^{Menth}CoCl$	[g]	318 (270, sh), 548 (44, sh), 592 (200, sh), 636 (330)	2474	638 (M^+, 7), 602 (100)	61.90 (62.12)	8.15 (8.22)	13.16 (13.17)
$Tp^{Menth}CuCl$	+189 ± 7 (1.1×10^{-3})	296 (1900), 376 (1600), 476 (380, sh), 737 (80), 1004 (70)	2474	643 (M^+, 10), 465 (100)	61.40 (61.68)	8.10 (8.16)	13.03 (13.08)
$Tp^{Menth}MnCl$	+204 ± 3 (1.7×10^{-3})	320 (280, sh)	2464	598 ([M − Cl]$^+$, 7), 367 (100)[f]	62.24 (62.57)	8.23 (8.27)	13.24 (13.27)
$Tp^{Menth}FeCl$	+271 ± 2 (2.7×10^{-3})	316 (330, sh)	2471	634 (M^+, 3), 367 (100)[f]	62.27 (62.48)	8.21 (8.26)	13.36 (13.25)
$Tp^{Menth}Cu(OAc)$	+220 ± 2 (1.9×10^{-3})	282 (3000), 772 (100)	2458	607 ([M − OAc]$^+$, 15), 429 (100)[f]	63.03 (63.10)	8.35 (8.32)	12.66 (12.62)
$Tp^{Menth}Ni(OAc)$	+267 ± 3 (1.8×10^{-3})	310 (330, sh), 430 (130), 708 (30)	2460	601 ([M − OAc]$^+$, 100)[f]	63.78 (63.56)	8.39 (8.38)	12.70 (12.71)
$Tp^{Menth}Cu(NO_3)$	+158 ± 1 (2.6×10^{-3})	268 (3200, sh), 288 (2000, sh), 796 (130)	2472	669 (M^+, 10), 135 (100)	59.63 (59.22)	7.85 (7.83)	14.80 (14.65)
$Tp^{Menth}Ni(NO_3)$	+244 ± 3 (2.0×10^{-3})	320 (520), 450 (120), 470 (121), 710 (40), 808 (40)	2472	601 ([M − NO_3]$^+$, 55), 367 (100)[f]	60.36 (59.66)	7.90 (7.89)	14.60 (14.76)
$Tp^{Menth}Rh(CO)_2$	+518 ± 9 (1.2×10^{-3})	286 (4800, sh), 366 (2700)	2478	703 ([M + H]$^+$, 75), 465 (100)[f]	59.36 (59.83)	7.37 (7.46)	11.93 (11.96)
$Tp^{Menth*}TiCl_3$	+398 ± 4 (2.1×10^{-3})[h]	340 (11,000), 416 (6600, sh)[h]	2490	661 ([M − Cl]$^+$, 4), 367 (100)[f,i]	56.49 (56.79)	7.67 (7.51)	11.79 (12.04)[j]

[a] Unless noted otherwise, all optical rotations were measured in $CHCl_3$ at the concentrations (g mL^{-1}) given in parentheses according to a published procedure (Dewey, M. A.; Gladysz, J. A. *Organometallics* **1993**, *12*, 2390−2397). [b] In CH_2Cl_2. [c] In cm^{-1}. [d] Unless noted otherwise, mass spectra used electron impact (EI) at 70 eV. [e] Calculated values given in parentheses. [f] Fast atom bombardment (FAB) MS data using MNBA matrix. [g] Unable to measure accurately due to significant absorption of the sodium D line radiation. [h] In THF. [i] Negative ion FAB-MS data: 696 (M^-, 7), 311 (100). [j] Analysis for Cl: 15.02 (15.24).

was extracted with toluene, and the extract was filtered through Celite. Concentration of the filtrate to ~1 mL and diffusion of MeOH into the blue toluene solution yielded the complex as blue crystals (0.25 g, 56% based on ligand; mp = 260−261 °C). Yields for complexes of Zn (mp = 256−257 °C), Ni (mp = 255−256 °C), and Cu (mp = 199−200 °C) were similar. $Tp^{Menth}ZnCl$: ^1H NMR ($CDCl_3$, 300 MHz) δ 7.39 (s, 3H), 2.68 (m, 6H), 2.05 (m, 3H), 1.94 (m, 3H), 1.71 (m, 3H), 1.58 (m, 3H), 1.37 (m, 3H), 1.16 (d, J = 6.8 Hz, 9H), 0.96 (d, J = 6.8 Hz, 9H), 0.85 (d, J = 6.7 Hz, 9H) ppm; $^{13}C\{^1H\}$ NMR ($CDCl_3$, 75 MHz) δ 153.6, 132.4, 120.9, 37.9, 31.7, 28.7, 27.0, 24.0, 22.1, 21.2, 19.7 ppm. $Tp^{Menth}CuCl$: EPR (9.1 GHz, 77 K, CH_2Cl_2/toluene glass) g_x = 2.01, g_y = 2.22, g_z = 2.40, A_x^{Cu} = 100 G.

$Tp^{Mementh}Zn^{II}Cl$. To a stirred solution of $ZnCl_2$ (0.155 g, 1.1 mmol) in THF (2 mL) at room temperature was added $TlTp^{Mementh}$ (0.300 g, 0.38 mmol) in THF (5 mL). A white precipitate immediately formed (TlCl), and after being stirred for 0.5 h, the mixture was filtered through Celite. The filtrate was concentrated to a white residue which was swirled in MeOH (20 mL). The precipitate which separated was collected by filtration, washed with MeOH, and dried. Recrystallization from toluene/MeOH afforded the product as a colorless solid (0.210 g, 81%). $Tp^{Mementh}ZnCl$: mp = 259−262 °C; ^1H NMR (CD_2Cl_2, 300 MHz) δ 7.36 (s, 3H), 2.94−2.80 (m, 3H), 2.48−2.60 (m, 3H), 1.71−1.84 (m, 12H), 1.05 (d, J = 6.9 Hz, 9H), 0.91 (m, 3H), 0.79 (s, 27H) ppm; $^{13}C\{^1H\}$ NMR (CD_2Cl_2, 75 MHz) δ 153.2, 131.5, 125.4, 40.8, 36.0, 33.0, 27.8, 27.4, 24.0, 21.3 ppm.

$Tp^{Menth}Fe^{II}Cl$. A mixture of $TlTp^{Menth}$ (1.09 g, 1.45 mmol) and $FeCl_2$ (0.189 g, 1.45 mmol) was stirred in CH_2Cl_2 (15 mL) for 12 h under a N_2 atmosphere. The mixture was then filtered, solvent was removed from the filtrate under vacuum, and the resulting solid was dissolved in Et_2O (~30 mL). When the mixture was allowed to stand at −20 °C, the product crystallized as colorless needles (0.56 g, 61%; mp = 184−186 °C).

$Tp^{Menth}Mn^{II}Cl$. The complex was prepared similarly to $Tp^{Menth}FeCl$, except that ~1.5 equiv of $MnCl_2 \cdot 4H_2O$ (0.250 g, 1.26 mmol for 0.661 g, 0.88 mmol of Tp^{Menth}) was used instead of equimolar $FeCl_2$, the reaction time was decreased to 3 h, and the crude product was washed with CH_3CN prior to Et_2O dissolution and crystallization (0.38 g, 68%; mp = 259−261 °C).

$Tp^{Menth}Cu^{II}(X)$ (X = OAc, NO_3) and $Tp^{Menth}Ni^{II}(NO_3)$. A similar procedure was used for the preparation of these three complexes, the only difference being the $M^{II}X_2$ source. The synthesis of $Tp^{Menth}Cu(NO_3)$ is typical: A solution of $TlTp^{Menth}$ (0.108 g, 0.144 mmol) in THF (1 mL) was added to a rapidly stirred solution of $Cu(NO_3)_2 \cdot 2.5H_2O$ (0.034 g, 0.144 mmol) in THF (1 mL). A white solid precipitated. After 15 min, solvent was removed under vacuum and the resulting residue was extracted with toluene (2 mL). The extracts were filtered,

Table 2. Crystallographic Data

	$Tp^{Menth}ZnCl$	$Tp^{Mementh}ZnCl$	$Tp^{Menth}Ni(OAc)$	$Tp^{Menth*}TiCl_3{\cdot}CH_2Cl_2$
formula	$C_{33}H_{52}BClN_6Zn$	$C_{36}H_{58}BClN_6Zn$	$C_{35}H_{55}BN_6NiO_2$	$C_{34}H_{54}BCl_5N_6Ti$
fw	644.46	686.54	661.37	782.82
space group	$P2_12_12_1$ (No. 19)	$P2_12_12_1$ (No. 19)	$P2_12_12_1$ (No. 19)	$P2_12_12_1$ (No. 19)
a (Å)	9.658(7)	11.170(4)	10.139(5)	10.335(8)
b (Å)	17.777(7)	14.829(9)	18.248(8)	15.430(7)
c (Å)	20.058(6)	23.063(9)	19.700(8)	25.11(1)
V (Å^3)	3444(5)	3820(5)	3645(5)	4004(7)
Z	4	4	4	4
ϱ_{calcd} (g cm^{-3})	1.243	1.194	1.205	1.298
μ (cm^{-1})	8.37	7.58	5.69	5.78
temp (°C)	−101	24	24	−100
radiation, λ (Å)	Mo Kα, 0.710 69	Mo Kα, 0.710 69	Mo Kα, 0.710 69	Mo Kα, 0.710 69
$2\theta_{max}$ (deg)	54.0	48.0	55.9	56.0
tot. no. of data collected	8260	6420	5158	7367
tot. no. of unique data[a]	6558	3396	4894	5388
tot. no. unique data with $I > 2\sigma(I)$	4055	4566	3721	3831
no. of variable params	379	407	406	424
R^b	0.063	0.055	0.043	0.070
$R_w{}^b$	0.049	0.056	0.039	0.071

[a] R_{int} values: 0.065 ($Tp^{Menth}ZnCl$); 0.069 ($Tp^{Mementh}ZnCl$); 0.018 ($Tp^{Menth}Ni(OAc)$); 0.123 ($Tp^{Menth*}TiCl_3{\cdot}CH_2Cl_2$). [b] $R = \sum||F_o| - |F_c||/\sum|F_o|$; $R_w = [\sum w(|F_o| - |F_c|)^2/\sum wF_o^2]^{1/2}$, where $w = 4F_o^2/s^2(F_o^2)$ and $s^2(F_o^2) = [S^2(C + R^2B) + pF_o^2)^2$, $(Lp)^2$ with S = scan rate, C = total integrated peak count, R = ratio of scan time to background counting time, B = total background count, Lp = Lorentz−polarization factor, and $p = p$ factor (0.03 for all except $Tp^{Menth*}TiCl_3{\cdot}CH_2Cl_2$, for which $p = 0.05$).

and the MeOH vapor was allowed to diffuse into the filtrate to give the product as green crystals (0.043 g, 49%; mp = 204−205 °C). $Tp^{Menth}Cu(OAc)$: mp = 205−207 °C; EPR (9.1 GHz, 77 K, CH_2Cl_2/toluene glass) $g_{||} = 2.33$, $g_\perp = 2.07$, $A_{||}^{Cu} = 137$ G, $A_\perp^N = 14$ G. $Tp^{Menth}Cu(NO_3)$: $g_{||} = 2.32$, $g_\perp = 2.07$, $A_{||}^{Cu} = 136$ G, $A_\perp^N = 13$ G. $Tp^{Menth}Ni(NO_3)$: mp = 261−262 °C.

$Tp^{Menth}Ni^{II}(OAc)$. To a solution of $Tp^{Menth}NiCl$ (0.114 g, 0.177 mmol) in CH_2Cl_2 (1.5 mL) was added NaOAc (0.073 g, 0.89 mmol), followed by dropwise addition of MeOH until the color changed sharply from dark brown to green and NaCl precipitation was evident. The mixture was stirred for 0.5 h and was filtered through Celite. Removal of solvent under reduced pressure followed by washing of the residue with MeOH afforded a green precipitate. Collection, drying, and recrystallization from toluene/methanol yielded the product as green crystals (0.096 g, 43%; mp = 229−230 °C).

$Tp^{Menth}Rh^{I}(CO)_2$. In a glovebox, $TlTp^{Menth}$ (0.101 g, 0.13 mmol) and $[Rh(CO)_2Cl]_2$ (26 mg, 0.13 mmol) were stirred in $CHCl_3$ (1.5 mL) for 15 min. The mixture was filtered through a Celite pad, and the filtrate was layered with CH_3NO_2 to yield the product as a yellow powder (0.019 g, 21%; mp = 145−153 °C dec: ^{1}H NMR ($CDCl_3$, 300 MHz, 0 °C) δ 7.73 (s, 1H), 7.56 (s, 1H), 7.42 (s, 2H), 6.39 (s, 1H), 3.1 (m, 1H), 2.67 (m, 8H), 2.41 (m, 4H), 1.8 (m, 12H), 1.4 (m, 5H), 1.1 (m, 30H), 0.8 (m, 8H), 0.77 (d, J = 6.4 Hz, 12H) ppm; ^{13}C{^{1}H} NMR ($CDCl_3$, 75 MHz, −20 °C) δ 184.9 (d, J_{RhC} = 67 Hz), 184.4 (d, J_{RhC} = 67 Hz), 154.41, 154.0, 153.0, 135.4, 133.5, 131.4, 123.6, 121.7, 121.6, 40.0, 39.2, 38.2, 32.6, 31.2, 30.2, 29.6, 29.1, 26.9, 26.5, 23.10, 22.5, 22.0, 21.7, 21.2, 20.5, 19.0, 18.8, 17.9 ppm; FTIR (ν_{CO}, KBr): 2079, 2059, 2012, 1987 cm^{-1}.

$Tp^{Menth*}Ti^{IV}Cl_3$. In a glovebox, titanium tetrachloride (25 mg, 0.13 mmol) in THF (4 mL) was added dropwise to a solution of $TlTp^{Menth}$ (100 mg, 0.13 mmol) in THF (10 mL). The resulting cloudy light yellow solution was stirred for 0.5 h, during which time it deepened to a dark red and deposited a precipitate (TlCl). The mixture was filtered through Celite, and solvent was removed from the filtrate in vacuo to afford a red solid, which was recrystallized from CH_2Cl_2/CH_3CN (39 mg, 0.056 mmol, 43% yield; mp = 182−185 °C): ^{1}H NMR (CD_2Cl_2, 300 MHz) δ 8.15 (s, 2H), 7.52 (s, 2H), 7.36 (s, 2H), 3.74 (m, 2H), 3.63 (m, 2H), 2.86−2.60 (m, 10H), 2.37 (m, 2H), 2.01 (m, 8H), 1.9−1.4 (m, 18H), 1.22 (d, J = 6.9 Hz, 6H), 1.21 (d, J = 7.2 Hz, 6H), 1.19 (d, J = 7.3 Hz, 6H), 0.948 (d, J = 7.0 Hz, 6H), 0.83−0.88 (m, 18H), 0.79 (d, J = 7.0 Hz, 6H), 0.74 (d, J = 6.7 Hz, 6H) ppm; ^{13}C{^{1}H} NMR (CD_2Cl_2, 125 MHz) δ 158.5, 157.8, 146.1, 142.5, 133.4, 132.2, 121.6, 121.2, 120.8, 38.3, 38.2, 37.1, 32.3, 31.3, 30.1, 28.3, 28.2, 27.8, 26.8, 26.6, 26.3, 24.2, 24.0, 23.7, 21.8, 21.6, 21.3, 21.1, 20.7, 20.3, 19.8, 19.7 ppm (32 out of 33 expected peaks observed).

$Tp^{Menth}Ti^{IV}Cl_3$. This complex was synthesized by the same procedure on the same scale as $Tp^{Menth*}TiCl_3$ except CH_2Cl_2 was used as solvent. Recrystallization yielded the product as an orange powder contaminated by ~10% $Tp^{menth*}TiCl_3$ by ^{1}H NMR (27 mg, 0.39 mmol, 30%; mp 178−182 °C): FTIR (KBr) 2487 (B−H) cm^{-1}; negative ion FAB-MS (MNBA matrix) (m/z) (relative intensity) 696 (M^-, 2), 543 (Tp^{Menth}, 20), 153 (100); ^{1}H NMR (CD_2Cl_2, 500 MHz) δ 7.49 (s, 3H), 3.74−3.76 (m, 3H), 2.70−2.75 (m, 3H), 2.52−2.57 (m, 3H), 2.02−2.05 (m, 3H), 1.75−1.79 (m, 3H), 1.65−1.70 (m, 3H), 1.48−1.53 (m, 3H), 1.22 (d, J = 7.0 Hz, 9H), 0.87 (d, J = 7.0 Hz, 9H), 0.78 (d, J = 7.5 Hz) ppm; ^{13}C{^{1}H} NMR (CD_2Cl_2, 125 MHz) δ 158.4, 132.3, 121.7, 38.4, 30.9, 28.0, 26.5, 23.9, 21.8, 20.7, 20.0 ppm.

X-ray Crystallography. A crystal of dimensions 0.60 × 0.50 × 0.20 mm^3 ($Tp^{Menth}ZnCl$, colorless), 0.50 × 0.35 × 0.35 mm^3 ($Tp^{Mementh}ZnCl$, colorless), 0.60 × 0.50 × 0.40 mm^3 ($Tp^{Menth}Ni(OAc)$, green), or 0.55 × 0.52 × 0.45 mm^3 ($Tp^{Menth*}TiCl_3{\cdot}CH_2Cl_2$, red) was mounted on a glass fiber with epoxy or oil and placed on an Enraf-Nonius CAD-4 diffractometer. Important crystallographic information is summarized in Table 2. Cell constants were obtained from a least-squares refinement of the setting angles of 23, 44, 24, or 22 carefully centered reflections in the range 17.02° < 2θ < 43.24°, 21.96° < 2θ < 37.21°, 42.06° < 2θ < 48.00°, or 19.50° < 2θ < 48.90°, respectively. The intensity data were collected using the $\omega-2\theta$ scan technique to the maximum 2θ values noted in Table 2. Empirical absorption corrections were applied using the program DIFABS[9] (except for $Tp^{Mementh}ZnCl$, where azimuthal scans of several reflections were used), which resulted in transmission factors ranging from 0.81 to 1.17, 0.89 to 1.00, 0.83 to 1.23, or 0.70 to 1.23, respectively. The data were corrected for Lorentz and polarization effects, but no decay corrections were needed. A correction for secondary extinction was applied to the structure of $Tp^{Mementh}ZnCl$ (coefficient = 1.4372 × 10^{-7}).

The structures were solved by direct methods[10] using the TEXSAN[11] software package. Non-hydrogen atoms were refined anisotropically, and the H atoms were placed at calculated positions. The maximum and minimum peaks on the final difference Fourier maps corresponded to 0.60 and −0.64 e/Å^3 for $Tp^{Menth}ZnCl$, 0.33 and −0.33 e/Å^3 for $Tp^{Mementh}ZnCl$, 0.25 and −0.28 e/Å^3 for $Tp^{Menth}Ni(OAc)$, and 0.43 and −0.48 e/Å^3 for $Tp^{Menth*}TiCl_3{\cdot}CH_2Cl_2$. Neutral-atom scattering factors and anomalous dispersion terms were taken from the literature.[12,13] The enantiomeric forms of the pyrazolyl rings were chosen by assuming

(9) Walker, N.; Stuart, D. *Acta Crystallogr.* **1983**, *A39*, 158−166.
(10) Calabrese, J. C. Ph.D. Thesis, University of Wisconsin, Madison, WI, 1972.
(11) *TEXSAN-Texray Structure Analysis Package*; Molecular Structure Corp.: The Woodlands, TX, 1985.
(12) Cromer, D. T. *International Tables for X-ray Crystallography*; The Kynoch Press: Birmingham, U.K., 1974; Vol. IV, Tables 2.2A and 2.3.1.
(13) Ibers, J. A.; Hamilton, W. C. *Acta Crystallogr.* **1964**, *17*, 781.

Table 3. Selected Positional Parameters and *B*(eq) Values (Excluding H Atoms)

atom	*x*	*y*	*z*	*B*(eq) (Å^2)	atom	*x*	*y*	*z*	*B*(eq) (Å^2)
				$Tp^{Menth}ZnCl$					
Zn1	0.06432(7)	0.03648(4)	−0.00253(5)	1.95(3)	C33	0.3718(7)	0.1157(4)	−0.1230(3)	2.1(3)
Cl1	−0.1413(2)	0.0603(1)	0.0354(1)	3.9(1)	C34	0.2816(8)	0.1701(4)	−0.1466(3)	2.2(3)
N11	0.2215(5)	0.0275(3)	0.0639(2)	1.7(2)	C35	0.1592(8)	0.1579(4)	−0.1131(3)	2.1(3)
N12	0.3483(6)	0.0161(3)	0.0342(3)	1.6(3)	C36	0.0266(8)	0.1996(4)	−0.1257(4)	3.2(4)
N21	0.1216(5)	−0.0622(3)	−0.0473(2)	1.7(2)	C37	0.045(1)	0.2537(4)	−0.1845(4)	4.1(5)
N22	0.2604(5)	−0.0643(3)	−0.0598(2)	1.5(2)	C38	0.191(1)	0.2880(4)	−0.1907(4)	4.6(5)
N31	0.1709(6)	0.0991(3)	−0.0704(3)	2.1(3)	C39	0.3052(9)	0.2311(4)	−0.1985(4)	3.2(4)
N32	0.3027(6)	0.0737(3)	−0.0781(3)	1.7(3)	C101	0.0654(8)	−0.0399(4)	0.1993(3)	3.0(3)
C13	0.4468(7)	0.0109(3)	0.0819(3)	1.8(3)	C102	0.044(1)	−0.0921(4)	0.1410(4)	4.4(5)
C14	0.3856(6)	0.0196(3)	0.1434(3)	1.5(3)	C103	−0.068(1)	−0.0243(5)	0.2373(4)	5.1(5)
C15	0.2462(6)	0.0279(4)	0.1297(3)	1.6(3)	C104	0.5394(9)	−0.0454(4)	0.2251(4)	4.1(4)
C16	0.1357(6)	0.0365(4)	0.1815(3)	2.1(3)	C201	−0.1644(7)	−0.1337(5)	−0.1152(3)	2.7(4)
C17	0.2063(8)	0.0727(4)	0.2416(3)	2.9(4)	C202	−0.1811(8)	−0.0498(5)	−0.1207(4)	4.0(4)
C18	0.3342(8)	0.0299(5)	0.2646(3)	3.2(4)	C203	−0.307(1)	−0.1706(5)	−0.1127(4)	4.6(5)
C19	0.4484(8)	0.0222(3)	0.2120(3)	2.1(3)	C204	0.2295(8)	−0.2764(4)	−0.1694(4)	3.6(4)
C23	0.2965(7()	−0.1327(4)	−0.0818(3)	1.6(3)	C301	−0.029(1)	0.2381(5)	−0.0630(5)	5.0(6)
C24	0.1794(7)	−0.1776(4)	−0.0837(3)	1.5(3)	C302	0.065(1)	0.3038(6)	−0.0383(4)	6.7(6)
C25	0.0718(7)	−0.1308(3)	−0.0619(3)	1.7(3)	C303	−0.175(1)	0.2681(6)	−0.0724(6)	8.9(8)
C26	−0.0754(8)	−0.1564(4)	−0.0550(3)	2.4(3)	C302	1.0357(8)	0.3671(6)	0.9561(4)	6.9(5)
C27	−0.0672(9)	−0.2416(4)	−0.0432(3)	2.9(4)	C303	0.8299(9)	0.4310(6)	0.9541(4)	8.7(6)
C28	0.0132(8)	−0.2823(4)	−0.0985(4)	3.0(4)	C304	0.9323(7)	0.3881(5)	0.8636(3)	6.1(4)
C29	0.1637(8)	−0.2596(4)	−0.1015(4)	2.6(4)	B1	1.0292(6)	0.0432(5)	0.7919(3)	3.1(3)
				$Tp^{Menth}Ni(OAc)$					
Ni1	0.06140(5)	0.03300(3)	0.10639(2)	2.34(2)	C26	0.1557(4)	−0.1641(2)	0.0926(2)	3.2(2)
O1	0.0118(3)	0.0782(2)	0.0116(1)	4.6(2)	C27	0.1261(5)	−0.2464(2)	0.1041(2)	4.5(2)
O2	0.1979(3)	0.0243(2)	0.0295(1)	4.5(1)	C28	0.1835(6)	−0.2796(2)	0.1683(2)	4.8(2)
N11	−0.1147(3)	0.0353(2)	0.1535(1)	2.5(1)	C29	0.1393(5)	−0.2427(2)	0.2340(2)	3.7(2)
N12	−0.1086(3)	0.0348(2)	0.2234(1)	2.6(1)	C33	0.1746(4)	0.1443(2)	0.2763(2)	2.8(2)
N21	0.1132(3)	−0.0537(2)	0.1663(1)	2.5(1)	C34	0.2421(4)	0.1917(2)	0.2361(2)	2.8(2)
N22	0.0914(3)	−0.0422(2)	0.2346(1)	2.5(1)	C35	0.2180(4)	0.1682(2)	0.1697(2)	2.5(2)
N31	0.1391(3)	0.1090(2)	0.1708(1)	2.4(1)	C36	0.2737(4)	0.2026(2)	0.1071(2)	3.1(2)
N32	0.1120(3)	0.0948(2)	0.2374(1)	2.5(1)	C37	0.3848(5)	0.2557(3)	0.1277(2)	4.4(2)
C1	0.1205(5)	0.0555(2)	−0.0108(2)	3.8(2)	C38	0.3558(5)	0.3008(3)	0.1897(3)	5.5(3)
C2	0.1584(7)	0.0657(3)	−0.0838(2)	7.3(3)	C39	0.3294(4)	0.2563(2)	0.2540(2)	3.9(2)
C13	−0.2317(4)	0.0358(2)	0.2486(2)	3.0(2)	C101	−0.2944(4)	−0.0401(3)	0.0303(2)	4.2(2)
C14	−0.3213(4)	0.0361(2)	0.1958(2)	3.0(2)	C102	−0.1676(6)	−0.0814(2)	0.0367(2)	5.0(2)
C15	−0.2444(3)	0.0353(2)	0.1375(2)	2.5(1)	C103	−0.3271(9)	−0.0318(4)	−0.0447(3)	10.6(4)
C16	−0.2974(4)	0.0347(2)	0.0661(2)	3.0(2)	C104	−0.5356(5)	−0.0021(3)	0.2509(3)	6.2(3)
C17	−0.4400(5)	0.0647(2)	0.0704(2)	4.3(2)	C201	0.2867(5)	−0.1472(2)	0.0571(2)	4.2(2)
C18	−0.5199(4)	0.0269(3)	0.1261(2)	4.6(2)	C202	0.2783(7)	−0.1641(3)	−0.0187(3)	8.1(4)
C19	−0.4690(4)	0.0435(2)	0.1966(2)	3.7(2)	C203	0.4068(5)	−0.1838(3)	0.0879(3)	6.9(3)
C23	0.1003(4)	−0.1065(2)	0.2678(2)	2.8(2)	C304	0.446(1)	0.2653(4)	−0.1935(5)	5.5(5)
C24	0.1294(4)	−0.1608(2)	0.2227(2)	2.8(2)	B1	0.356(1)	0.0025(5)	−0.0420(4)	1.7(4)
C25	0.1360(4)	−0.1264(2)	0.1599(2)	2.6(2)					
				$Tp^{Mementh}ZnCl$					
Zn1	0.84117(6)	0.18337(5)	0.77953(3)	3.71(3)	C33	1.0483(5)	0.0708(4)	0.9014(3)	3.5(3)
Cl1	0.7105(2)	0.2888(2)	0.7670(1)	7.8(1)	C34	0.9950(5)	0.1269(4)	0.9408(2)	3.5(3)
N11	0.8031(4)	0.0495(3)	0.7851(2)	3.6(2)	C35	0.9336(5)	0.1919(5)	0.9080(2)	3.4(3)
N12	0.9056(4)	−0.0012(3)	0.7811(2)	3.5(2)	C36	0.8577(6)	0.2667(4)	0.9318(3)	3.8(3)
N21	0.9727(4)	0.1632(3)	0.7196(2)	4.1(2)	C37	0.8250(9)	0.2410(6)	0.9954(4)	6.8(5)
N22	1.0569(4)	0.1033(4)	0.7394(2)	3.6(2)	C38	0.853(1)	0.1521(8)	1.0172(4)	11.0(7)
N31	0.9478(4)	0.1731(4)	0.8511(2)	3.4(2)	C39	0.9781(7)	0.1176(6)	1.0057(3)	4.9(4)
N32	1.0202(4)	0.0998(3)	0.8476(2)	3.2(2)	C40	0.9137(6)	0.3608(5)	0.9263(3)	4.3(3)
C13	0.8780(6)	−0.0839(4)	0.7617(2)	3.7(3)	C101	0.7497(7)	−0.2181(6)	0.6817(4)	6.6(5)
C14	0.7561(5)	−0.0892(5)	0.7521(3)	3.6(3)	C102	0.3921(7)	0.0497(7)	0.8242(4)	8.2(6)
C15	0.7143(5)	−0.0043(4)	0.7680(3)	3.5(3)	C103	0.542(1)	−0.0576(9)	0.8615(4)	10.6(7)
C16	0.5827(6)	0.0226(5)	0.7670(3)	4.3(3)	C104	0.5845(7)	0.1048(8)	0.8621(4)	8.8(6)
C17	0.5132(7)	−0.0426(6)	0.7274(4)	7.1(5)	C201	1.3339(9)	0.1756(6)	0.6168(3)	7.8(5)
C18	0.5838(7)	−0.1033(7)	0.6895(4)	7.2(5)	C202	0.7778(9)	0.2899(7)	0.5614(4)	8.8(6)
C19	0.6806(6)	−0.1582(4)	0.7228(3)	4.9(3)	C203	0.902(1)	0.1483(7)	0.5493(4)	9.9(7)
C20	0.5270(6)	0.0282(6)	0.8285(4)	5.7(4)	C204	0.7600(9)	0.1637(7)	0.6310(4)	9.1(6)
C23	1.1482(6)	0.1010(4)	0.7015(2)	3.8(3)	C301	0.987(1)	0.0208(7)	1.0251(3)	7.7(5)
C24	1.1257(6)	0.1584(4)	0.6566(3)	4.0(3)	C204	0.2272(7)	−0.2624(3)	0.2933(3)	6.4(3)
C25	1.0140(6)	0.1956(5)	0.6686(2)	3.8(3)	C301	0.1670(5)	0.2353(2)	0.0598(2)	3.7(2)
C26	0.9480(7)	0.2602(5)	0.6309(3)	4.9(4)	C302	0.2257(6)	0.2532(3)	−0.0105(3)	6.1(3)
C27	1.041(1)	0.3124(6)	0.5926(3)	7.2(5)	C303	0.0947(6)	0.3014(3)	0.0884(3)	6.0(3)
C28	1.173(1)	0.2921(5)	0.6021(3)	6.6(5)	C304	0.2693(6)	0.3039(3)	0.3089(3)	6.0(3)
C29	1.2011(7)	0.1920(6)	0.6071(3)	5.3(4)	B1	0.0253(4)	0.0294(3)	0.2581(2)	2.6(2)
C30	0.847(1)	0.2152(6)	0.5934(3)	6.6(4)					
				$Tp^{Menth*}TiCl_3{\cdot}CH_2Cl_2$					
Ti1	0.7667(1)	0.16927(8)	0.74001(6)	2.31(5)	C27	0.520(1)	0.4548(6)	0.5678(4)	3.9(2)
Cl1	0.5762(2)	0.1004(1)	0.75583(8)	3.02(8)	C28	0.505(1)	0.3790(6)	0.5287(4)	5.2(5)
Cl2	0.8862(2)	0.1098(1)	0.80492(8)	2.94(8)	C29	0.482(1)	0.2915(6)	0.5574(4)	4.6(5)

Table 3 (Continued)

Cl3	0.8270(3)	0.0731(1)	0.67715(9)	3.58(9)	C30	0.772(1)	0.4575(6)	0.5689(4)	3.8(4)
N11	0.9196(7)	0.2576(4)	0.7214(3)	2.5(3)	C33	0.5950(8)	0.3967(5)	0.7974(3)	2.5(3)
N12	0.8967(7)	0.3456(4)	0.7253(2)	2.3(2)	C34	0.5533(8)	0.3476(5)	0.8415(3)	2.5(3)
N21	0.6945(6)	0.3301(4)	0.6731(2)	2.3(2)	C35	0.6270(8)	0.2726(5)	0.8377(3)	2.5(3)
N22	0.6692(7)	0.2439(4)	0.6810(3)	2.6(3)	C36	0.6272(9)	0.2008(5)	0.8790(3)	2.5(3)
N31	0.7046(7)	0.2728(4)	0.7937(2)	2.3(3)	C37	0.499(1)	0.2104(6)	0.9108(4)	3.8(4)
N32	0.6834(7)	0.3524(4)	0.7702(2)	2.2(2)	C38	0.460(1)	0.3026(6)	0.9279(4)	3.8(4)
C13	1.0102(8)	0.3885(5)	0.7321(3)	2.6(3)	C39	0.4496(9)	0.3654(6)	0.8814(3)	3.1(4)
C14	1.1105(9)	0.3291(6)	0.7319(3)	2.9(3)	C40	0.755(1)	0.2022(5)	0.9127(3)	3.0(3)
C15	1.0524(8)	0.2493(5)	0.7232(3)	2.6(3)	C101	1.309(1)	0.3963(6)	0.6936(4)	3.8(4)
C16	1.1268(8)	0.1667(5)	0.7163(3)	2.8(3)	C102	1.229(2)	0.070(1)	0.6496(5)	9(1)
C17	1.242(1)	0.1763(5)	0.7562(4)	3.8(4)	C103	1.101(2)	0.1926(8)	0.6153(5)	7.5(8)
C18	1.326(1)	0.2563(5)	0.7459(5)	4.7(5)	C201	0.496(2)	0.2157(7)	0.5202(5)	7.5(8)
C19	1.2536(8)	0.3431(5)	0.7392(4)	3.2(3)	C202	0.775(2)	0.5465(8)	0.5432(6)	9(1)
C20	1.175(1)	0.1593(8)	0.6577(4)	6.0(6)	C203	0.894(1)	0.4413(8)	0.5993(5)	5.2(6)
C23	0.5967(9)	0.2188(5)	0.6397(3)	2.8(3)	C301	0.446(1)	0.4598(6)	0.9002(4)	4.2(5)
C24	0.571(1)	0.2859(5)	0.6053(3)	3.5(4)	C302	0.769(1)	0.1152(5)	0.9413(4)	4.0(4)
C25	0.636(1)	0.3553(5)	0.6268(3)	3.1(4)	C303	0.767(1)	0.2769(5)	0.9519(3)	3.3(4)
C26	0.645(1)	0.4443(5)	0.6021(3)	3.1(4)	B1	0.759(1)	0.3785(5)	0.7196(4)	2.5(3)

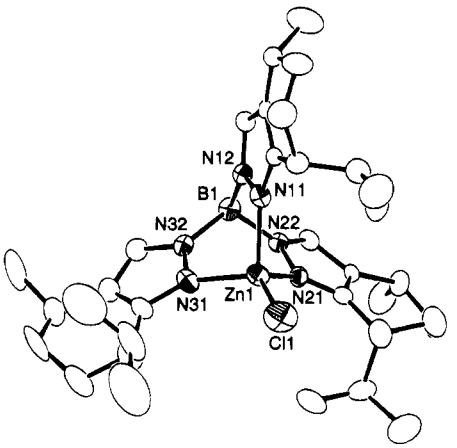

Figure 1. ORTEP representation of the X-ray structure of Tp^{Menth}-ZnCl showing 60% probability ellipsoids for all non-hydrogen atoms (carbon atoms not labeled for clarity). Selected interatomic distances (Å) and angles (deg): Zn1−Cl1, 2.168(2); Zn1−N11, 2.026(5); Zn1−N21, 2.047(5); Zn1−N31, 2.037(6); Cl1−Zn1−N11, 118.1(2); Cl1−Zn1−N21, 124.6(2); Cl1−Zn1−N31, 126.2(2); N11−Zn1−N21, 91.0(2); N11−Zn1−N31, 96.0(2); N21−Zn1−N31, 92.2(2).

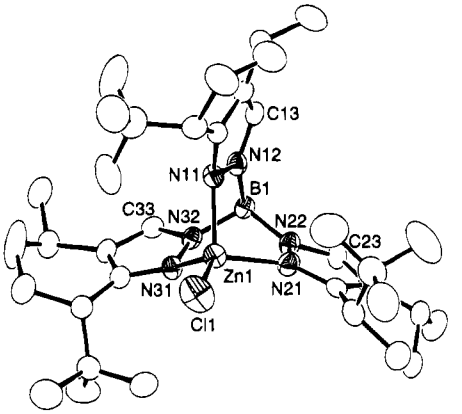

Figure 2. ORTEP representation of the X-ray structure of $Tp^{Mementh}$-ZnCl showing 35% probability ellipsoids for all non-hydrogen atoms (most of the carbon atoms are not labeled for clarity). Selected interatomic distances (Å) and angles (deg): Zn1−Cl1, 2.158(2); Zn1−N11, 2.035(5); Zn1−N21, 2.039(5); Zn1−N31, 2.040(5); Cl1−Zn1−N11, 125.0(1); Cl1−Zn1−N21, 120.2(2); Cl1−Zn1−N31, 123.9(2); N11−Zn1−N21, 92.9(2); N11−Zn1−N31, 89.9(2); N21−Zn1−N31, 96.7(2).

that the absolute configuration at the 4-position of the six-membered ring (containing the methyl group) remained unchanged from the ligand.[6] This assumption was checked in the cases of $Tp^{Menth}ZnCl$, $Tp^{Mementh}ZnCl$, and $Tp^{Menth}Ni(OAc)$ by carrying out refinement of the X-ray data with the opposite enantiomer; convergence was reached with significantly higher values for R, R_w, and goodness of fit in each case. Drawings of the structures appear in Figures 1−5, with selected bond lengths and angles listed in the figure captions. Selected final atomic positional parameters and B(eq) values (excluding those for H atoms) are listed in Table 3. Completely labeled ORTEP drawings and full tables of bond lengths and angles, atomic positional parameters, and final thermal parameters for non-hydrogen atoms are given for $Tp^{Mementh}$-ZnCl, $Tp^{Menth}Ni(OAc)$, and Tp^{Menth}*$TiCl_3$*CH_2Cl_2 in the supplementary material (Figures S1−S3 and Tables S1−S12) and for $Tp^{Menth}ZnCl$ in the supplementary material of a preliminary communication.[5]

Results and Discussion

Four-Coordinate Tp*$M^{II}Cl$ (M^{II} = Zn^{II}, Ni^{II}, Co^{II}, Cu^{II}, Mn^{II}, Fe^{II}) Complexes. Metathesis reactions between $TlTp^{Menth}$ or $TlTp^{Mementh}$ and the appropriate divalent metal halide resulted in the formation of Tp*MCl complexes (Tp* = Tp^{Menth} or $Tp^{Mementh}$), all of which were isolated as crystalline or microcrystalline solids. This synthetic method, which relies on access to the Tl^I salts of the chiral ligands,[6] is more straightforward than our previously communicated procedure starting with crude solutions of KTp^{Menth} contaminated with free pyrazole.[5] The

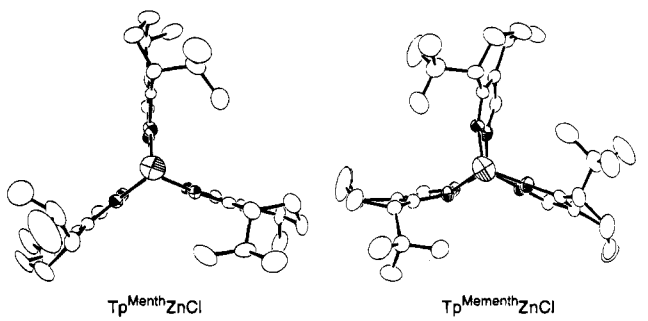

Figure 3. Views of the X-ray crystal structures of $Tp^{Menth}ZnCl$ (left) and $Tp^{Mementh}ZnCl$ (right) along their respective Cl−Zn bonds.

specific, nonstoichiometric ratios of TlTp* to metal salt used in these syntheses, as well as the other syntheses discussed below, were found to be optimal for obtaining high yields of the desired complexes. The lack of Tp_2M "sandwich" products in these preparations testifies to the steric bulk of the chiral ligands, which appears similar to that of Tp^{iPr2} and Tp^{tBu} on the basis of the analogous lack of Tp_2M complexes in metathesis reactions of salts of these achiral chelates with metal halides.[14-19]

Spectroscopic and physical data, listed in Table 1, support 4-coordinate, C_3-distorted pseudotetrahedral structural formula-

(14) Trofimenko, S.; Calabrese, J. C.; Thompson, J. S. *Inorg. Chem.* **1987**, *26*, 1507−1514.

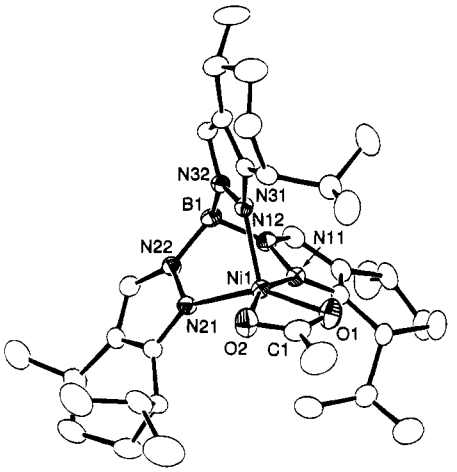

Figure 4. ORTEP representation of the X-ray structure of $Tp^{Menth}Ni(OAc)$ showing 35% probability ellipsoids for all non-hydrogen atoms (carbon atoms not labeled for clarity). Selected interatomic distances (Å) and angles (deg): Ni1–O1, 2.102(3); Ni1–O2, 2.058(3); Ni1–N11, 2.014(3); Ni1–N21, 2.042(3); Ni1–N31, 2.038(3); O1–C1, 1.257(5); O2–C1, 1.254(5); O1–Ni1–O2, 62.5(1); O1–Ni1–N11, 100.9(1); O1–Ni1–N21, 151.5(1); O1–Ni1–N31, 112.2(1); O2–Ni1–N11, 159.7(1); O2–Ni1–N21, 101.1(1); O2–Ni1–N31, 104.5(1); N11–Ni1–N21, 88.7(1); N11–Ni1–N31, 92.4(1); N21–Ni1–N31, 93.9(1); O1–C1–O2, 118.4(4).

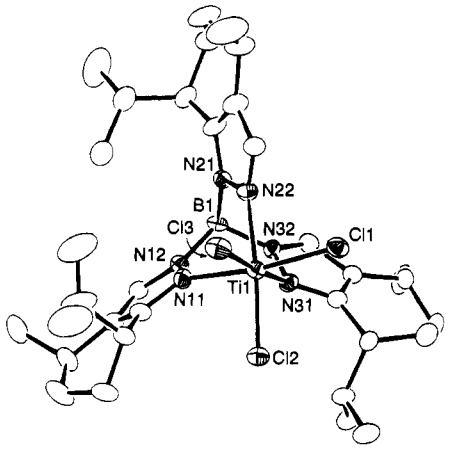

Figure 5. ORTEP representation of the X-ray structure of $Tp^{Menth*}TiCl_3{\cdot}CH_2Cl_2$ showing 40% probability ellipsoids for all non-hydrogen atoms (CH_2Cl_2 not shown and carbon atoms not labeled for clarity). Selected interatomic distances (Å) and angles (deg): Ti1–Cl1, 2.272(3); Ti1–Cl2, 2.242(3); Ti1–Cl3, 2.255(3); Ti1–N11, 2.139(7); Ti1–N22, 2.131(7); Ti1–N31, 2.186(6); Cl1–Ti1–Cl2, 99.1(1); Cl1–Ti1–Cl3, 93.1(1); Cl1–Ti1–N11, 167.5(2); Cl1–Ti1–N22, 88.0(2); Cl1–Ti1–N31, 88.8(2); Cl2–Ti1–Cl3, 95.0(1); Cl2–Ti1–N11, 90.7(2); Cl2–Ti1–N22, 171.2(2); Cl2–Ti1–N31, 90.7(2); Cl3–Ti1–N11, 93.6(2); Cl3–Ti1–N22, 90.0(2); Cl3–Ti1–N31, 173.6(2); N11–Ti1–N22, 81.6(3); N11–Ti1–N31, 83.4(2); N22–Ti1–N31, 84.0(2).

tions for the Tp*MCl compounds closely analogous to those of their previously reported C_{3v}-symmetric Tp^{iPr2} and/or Tp^{tBu} congeners, several of which have been characterized by X-ray crystallography.[16–19] Despite apparent discrepancies with values cited for some Tp^{iPr2} and Tp^{tBu} analogs,[20] the position and intensity of the dd bands in the UV–vis spectra of $Tp^{Menth}M^{II}Cl$ ($M = Ni^{II}$, Co^{II}, Cu^{II}) implicates tridentate binding of the polypyrazolyl ligand to yield pseudotetrahedral metal ion geometries (Ni λ_{max} = 806 nm, ϵ = 80 M^{-1} cm^{-1}; Co λ_{max} = 636, ϵ = 330 M^{-1} cm^{-1}; Cu λ_{max} = 737 and 1004 nm, ϵ = 80 and 70 M^{-1} cm^{-1}). Observation of a rhombic signal with large metal-derived hyperfine splitting in the high-field component of the EPR spectrum of a frozen CH_2Cl_2–toluene solution of the Cu complex (g_x = 2.01, g_y = 2.22, g_z = 2.40, A_x^{Cu} = 100 G) further supports a C_3-symmetric 4-coordinate structural assignment for this species. Similar EPR parameters were previously identified for $Tp^{tBu}CuCl$[8,21] and $Tp^{iPr2}CuCl$[19] in comparable nondonor solvents; in THF or DMF, axial signals indicative of solvent coordination to yield square pyramidal species were observed for the latter complex.[10] Finally, we observed single sets of pyrazolyl ring resonances in the ^1H and ^{13}C NMR spectra of $Tp^{Menth}ZnCl$ and $Tp^{Mementh}ZnCl$, consistent with C_3-symmetric structures for these complexes in solution.

These spectroscopy-based structural hypotheses for the Zn compounds were confirmed by X-ray crystallographic studies (Figures 1–3). Positional parameters are listed in Table 3. Both $Tp^{Menth}ZnCl$ and $Tp^{Mementh}ZnCl$ exhibit tridentate binding of the respective Tp* ligand with acute N_{pz}–Zn–N_{pz} and correspondingly obtuse N_{pz}–Zn–Cl angles (average N_{pz}–Zn–N_{pz} = 93°; average N_{pz}–Zn–Cl = 123°) that are typical for TpMX complexes.[2] The unexceptional Zn–N and Zn–Cl bond lengths (average Zn–N = 2.04 Å; average Zn–Cl = 2.16 Å) are similar to those cited by Yoon and Parkin for $Tp^{tBu}ZnCl$.[18] Most intriguing is the nature of the chiral pocket enclosed by the substituents of the Tp* ligands in each of the complexes, which is comparable in each instance to that uncovered in the previously reported X-ray structures of the respective Tl^I precursors.[6] As is most evident in the views along the Zn···B–H axes shown in Figure 3, the opposite absolute configurations of the *i*-Pr- and *t*-Bu-substituted carbons of the Tp^{Menth} and $Tp^{Mementh}$ ligands, respectively, result in opposite rotational symmetries in the Zn^{II} complexes (clockwise vs counterclockwise arrangement of *i*-Pr and *t*-Bu groups, respectively). Interestingly, there appears to be an empirical correlation between the sign of the large specific rotations of the $Tp^{Menth}M$ and $Tp^{Mementh}$ (M = Tl^I and Zn^{II}) complexes (Table 1 and ref 6) and their rotational stereochemistries (positive α_D for Tp^{Menth} vs negative α_D for $Tp^{Mementh}$).

In the X-ray structure of $TlTp^{Mementh}$ reported recently we noted an unusual, severe "propeller-like" distortion of the tris(pyrazolyl) unit that we ascribed to steric interactions among the *t*-Bu groups.[6] This distortion,[22] which resulted in a lack of coincidence of the bonding lone pairs on the N_{pz} atoms with their N–Tl bonds that we suggested might reflect ionic character in the bonding, occurs to a lesser extent in $Tp^{Mementh}ZnCl$. This is indicated by the Zn1–N11–N12–C13, Zn1–N21–N22–C23, and Zn1–N31–N32–C33 torsion angles [155.3(4), 172.6-

(15) Kitajima, N.; Hikichi, S.; Tanaka, M.; Moro-oka, Y. *J. Am. Chem. Soc.* **1993**, *115*, 5496–5508.
(16) Gorrell, I. B.; Parkin, G. *Inorg. Chem.* **1990**, *29*, 2452–2456.
(17) Han, R.; Looney, A.; McNeill, K.; Parkin, G.; Rheingold, A. L.; Haggerty, B. S. *J. Inorg. Biochem.* **1993**, *49*, 105–121.
(18) Yoon, K.; Parkin, G. *J. Am. Chem. Soc.* **1991**, *113*, 8414–8418.
(19) Kitajima, N.; Fujisawa, K.; Moro-oka, Y. *J. Am. Chem. Soc.* **1990**, *112*, 3210–3212.
(20) The absorption features of $Tp^{Menth}NiCl$ in CH_2Cl_2 (Table 1) are similar to those reported for $Tp^{iPr2}NiCl$ in toluene [λ_{max} (ϵ) = 400 (230), 801 (110) nm[19]] but different from those for $Tp^{tBu}NiCl$ in THF [λ_{max} (ϵ) = 505 (43) nm[17]]. The spectrum of $Tp^{Menth}NiCl$ in THF [λ_{max} (ϵ) = 486 (320), 552 (80, sh), 802 (80) nm] is also different from that of its Tp^{tBu} analog, a puzzling observation which, nonetheless, suggests THF coordination in this solvent. Similar THF binding to $Tp^{Menth}CoCl$ is indicated by the differences between UV–vis spectra measured in CH_2Cl_2 (Table 1) and in THF [λ_{max} (ϵ) = 556 (90, sh), 596 (380, sh), 630 (570), 652 (540, sh) nm], the latter of which closely match data reported for $Tp^{tBu}CoCl$ in the same solvent [λ_{max} (ϵ) = 547 (370), 603 (316), 633 (496), 659 (417) nm[17]].
(21) Tolman, W. B.; Carrier, S. M.; Ruggiero, C. E.; Antholine, W. E.; Whittaker, J. W. In *Bioinorganic Chemistry of Copper*; Karlin, K. D., Tyeklár, Z., Eds.; Chapman & Hall, Inc.: New York, 1993; pp 406–418.
(22) Similar distortions are apparent in some other $TlTp^{RR'}$ crystal structures. For example, see: Libertini, E.; Yoon, K.; Parkin, G. *Polyhedron* **1993**, *12*, 2539–2542.

(4), and 152.8(4)°, respectively] that are less perturbed from the ideal 180° angle than in the Tl^{I} complex [159.5(7), 139.9(9), and 142.4(9)° for the like angles]. We speculate that greater covalency in the bonding of $Tp^{Mementh}$ to the Zn^{II} ion may counteract the steric repulsions that induce the distortion in the more ionic Tl^{I} species. The "propeller" distortion is not apparent in the less sterically hindered $Tp^{Menth}ZnCl$, which, like its $TlTp^{Menth}$ precursor,[6] exhibits torsion angles that are essentially equal to 180° [179.9(4), 172.9(4), and 179.9(4)°].

Five-Coordinate $Tp^{Menth}M(NO_3)$ and $Tp^{Menth}M(OAc)$ (M = Cu, Ni). With the exception of $Tp^{Menth}Ni(OAc)$, which was best prepared by exchange of the chloride ligand of $Tp^{Menth}NiCl$ with the acetate ion, these complexes were synthesized by metathesis of $TlTp^{Menth}$ with the appropriate metal(II) acetate or nitrate. We conclude that symmetrical bidentate coordination of nitrate and acetate occurs to afford 5-coordinate $Tp^{Menth}M$ (M = Cu, Ni) complexes on the basis of the close similarity of their UV−vis spectral features with those of structurally characterized $Tp^{tBu}M(\eta^2\text{-}O_2NO)$[17] or $Tp^{iPr2}Cu(m\text{-chlorobenzoate})$,[23] as well as $Tp^{tBu}Cu(OAc)$.[24] In addition, square pyramidal metal ion geometries for the Cu^{II} complexes are supported by the presence of axial signals in their EPR spectra [$Tp^{Menth}Cu(OAc)$ $g_{\|} = 2.33$, $g_{\perp} = 2.07$, $A_{\|}^{Cu} = 137$ G, $A_{\perp}^{N} = 14$ G; $Tp^{Menth}Cu(NO_3)$ $g_{\|} = 2.32$, $g_{\perp} = 2.07$, $A_{\|}^{Cu} = 136$ G, $A_{\perp}^{N} = 13$ G].

The pentacoordinate formulation for $Tp^{Menth}Ni(OAc)$ was confirmed by X-ray crystallography (Figure 4; positional parameters in Table 3). Except for a slight deviation from ideal symmetric coordination of acetate [$\Delta(Ni-O) = 0.044$ Å] and a lack of a mirror plane due to the chirality of the Tp^{Menth} ligand, the bond lengths and angles in the Ni^{II} coordination sphere of $Tp^{Menth}Ni(OAc)$ are essentially identical to those reported for $Tp^{tBu}Ni(NO_3)$.[17] The geometry of both complexes can be described as distorted square pyramidal; for $Tp^{Menth}Ni(OAc)$, angles subtended by the N31−Ni1 bond and the bonds between Ni1 and the remaining donor atoms that are only moderately distorted from the ideal of 90° suggest that N31 occupies the pseudoaxial position [$N31-Ni1-O_{acetate} = 104.5(1)$ and 112.2(1)°; $N31-Ni1-N_{pz} = 92.4(1)$ and 93.9(1)°].

$Tp^{Menth}Rh(CO)_2$. This complex, which was targeted because of its potential utility in stereospecific C−H bond activation processes,[25] was isolated from the reaction of $[Rh(CO)_2Cl]_2$ with $TlTp^{Menth}$ in $CHCl_3$ via a procedure analogous to that used by other workers to prepare the series $Tp^{RR'}Rh(CO)_2$ (R = *t*-Bu, *i*-Pr, or Ph, R′ = H; R = CF_3, R′ = Me; R = R′ = Me; R = 3-pyrazolyl and R′ = 5-pyrazolyl substituents).[26,27] Like those for most of the latter series of complexes, the combined IR and NMR data for $Tp^{Menth}Rh(CO)_2$ indicate that the complex exists as an approximate 1:1 mixture of isomers. One is a 5-coordinate, formally 18-electron complex with η^3-coordination of Tp^{Menth}, and the second is four-coordinate with 16 electrons and an η^2-Tp^{Menth} ligand (Scheme 1). Four ν_{CO} bands of approximately equal intensity are evident in the infrared spectrum (KBr) of the complex, a sharp pair (2079 and 2012 cm^{-1}) and a broader set at lower energy (2059 and 1987 cm^{-1}). By comparison to the extensive data reported for $Tp^{RR'}Rh(CO)_2$,[26] we assign the former features to the 4-coordinate form and the latter bands to the more electron rich 5-coordinate isomer [cf.: η^2-$Tp^{iPr}Rh(CO)_2$ (2082, 2017 cm^{-1}; η^3-$Tp^{iPr}Rh(CO)_2$ 2058, 1987 cm^{-1}]. The ^1H NMR spectrum at 22 °C in CD_2Cl_2 is broad and difficult to interpret, but upon cooling to 0 °C a sharp spectrum is obtained which exhibits two sets of resonances, one with a single 5-pyrazolyl hydrogen peak and the other with three such peaks in a 1:1:1 ratio. We attribute the latter pattern to η^2-$Tp^{Menth}Rh(CO)_2$, which would be expected to have three inequivalent pyrazolyl rings (C_1 symmetry), and the former resonance to the 5-coordinate η^3-Tp^{Menth} form, in which rapid averaging of pyrazolyl ring environments occurs via pseudorotation or turnstile processes. Analogous NMR spectral data were reported for the series $Tp^{RR'}Rh(CO)_2$,[26] and X-ray crystallographic support for the existence of the η^2 forms was obtained for several compounds from this set.[28,29] It has also been noted that the η^2:η^3 ratio largely depends on the size of the 3-pyrazolyl substituents, with, for example, the largest (*t*-Bu) inducing exclusive formation of the η^2 isomer and the much smaller Me group causing generation of the η^3 form only.[26] The ~1:1 ratio (~3:2 by NMR at 0 °C) we observe for Tp^{Menth} thus implies steric hindrance between that of Tp^{tBu} and Tp^{Me2}, similar to Tp^{iPr} (35:65 η^2:η^3 ratio in cyclohexane).[26]

Scheme 1

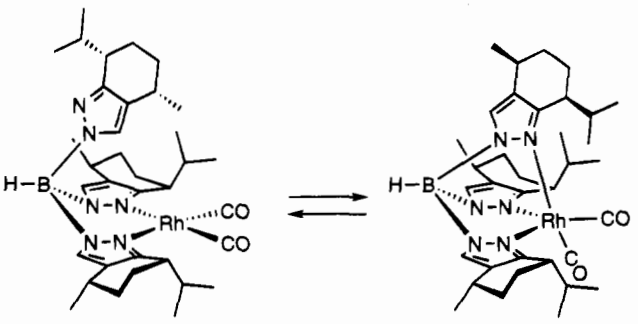

Six-Coordinate $Tp^{*}TiCl_3$ Complexes. Depending on the reaction solvent, one of two different isomeric complexes was formed upon treatment of $TlTp^{Menth}$ with $TiCl_4$. When CH_2Cl_2 was used, spectroscopic and MS data of the product isolated indicated that it contained predominantly $Tp^{Menth}TiCl_3$ contaminated with ~10% of the other isomer (*vide infra*). Thus, the appropriate parent ion in the negative-ion FAB mass spectrum, a single ν_{BH} in the IR spectrum, and a single set of resonances in the ^1H and ^{13}C NMR spectra are consistent with a C_3-symmetric, presumably octahedral, major product. Attempts to purify the complex and conclusively characterize its structure have met with failure, however, in part because of its tendency to isomerize to the other isomer when dissolved in THF.

The properties of this second isomer, $Tp^{Menth*}TlCl_3$, which formed exclusively when the preparative reaction was carried out in THF and which was thus isolated pure, are summarized in Table 1. The presence of three sets of pyrazolyl peaks in a 1:1:1 ratio in its ^1H NMR spectrum and 32 separate resonances in its ^{13}C NMR spectrum (out of an expected 33, with some spectral overlap) suggests that the pyrazolyl ring environments are inequivalent in this complex. This inequivalence is apparent in the X-ray crystal structure shown in Figure 5 (positional parameters in Table 3), which reveals that the Tp^{Menth} ligand has isomerized to an asymmetric form (Tp^{Menth*}) with one pyrazolyl ring bound via its less (instead of more) hindered N atom to the octahedral Ti^{IV} ion. Other $Tp^{RR'}Ti^{IV}Cl_3$ (R = R′ = H or Me) complexes have been reported,[30,31] but to our knowledge, the only TpTi complexes to be structurally char-

(23) Kitajima, N.; Fujusawa, K.; Moro-oka, Y. *Inorg. Chem.* **1990**, *29*, 357−358.
(24) Tolman, W. B. *Inorg. Chem.* **1991**, *30*, 4878−4880.
(25) Ghosh, C. K.; Graham, W. A. G. *J. Am. Chem. Soc.* **1987**, *109*, 4726−4727.
(26) Krentz, R. Ph.D. Thesis, University of Alberta, 1989.
(27) May, S.; Reinsalu, P.; Powell, J. *Inorg. Chem.* **1980**, *19*, 1582−1589.
(28) Ball, R. G. Structure Determination Laboratory Report No. SR:071801-12-87, University of Alberta, 1989; quoted in ref 26.
(29) Cowie, M.; Ball, R. G. Unpublished results, University of Alberta, 1989; quoted in ref 26.
(30) Manzer, L. E. *J. Organomet. Chem.* **1975**, *102*, 167−174.

acterized are Ti^{III} variants [$TpTiCl_2$(3,5-Me_2pzH) and ($NHMe_2NHMe$)($TpTiCl_3$)][32] and 7-coordinate $TpTi^{IV}Cl_2$-($RNNR_2$)[33] species. As expected from the lower coordination number of $Tp^{Menth*}TiCl_3$, its Ti−N_{pz} and Ti−Cl bond lengths (average 2.15 and 2.26 Å, respectively) are shorter than those in the latter 7-coordinate compounds (average 2.20 and 2.35 Å for the R = Me).[33] These distances in $Tp^{Menth*}TiCl_3$ are also shorter than the analogous bond lengths in the Ti^{III} complexes [$TpTi^{III}Cl_3^-$, 2.34 and 2.40 Å; $TpTi^{III}Cl_2$(3,5-Me_2pzH), average 2.18 and 2.36 Å].[32]

Rearrangements analogous to $Tp^{Menth}TiCl_3 \rightarrow Tp^{Menth*}TiCl_3$ have been reported for $Tp^{RR'}$ and bis(pyrazolyl)hydroborate ligands, although in most instances such "borotropic shifts" occur under more drastic (high temperature) conditions.[34-39] As in most of these other cases, alleviation of steric strain resulting from the bulky pyrazolyl 3-substituents appears to be the underlying rationale for the rearrangement of $Tp^{Menth}TiCl_3$ to its less symmetric (but thermodynamically more stable) isomer.[40] In the absence of detailed mechanistic information, we can only speculate that the facility of this borotropic shift may be the result of efficient B−N bond cleavage by the highly Lewis-acidic Ti^{IV} ion.

Conclusions

The versatile binding properties of the chiral Tp* ligands have been demonstrated by our isolation and full characterization of a wide range of their complexes with different transition metals having divergent geometries and formal oxidation states. This versatility is an important prerequisite for the rational development of new enantioselective processes using Tp*M species as catalysts or promotors. The combined synthetic, spectroscopic, and structural data for the complexes we have synthesized suggest that the Tp* ligands have effective steric properties between those of the achiral variants with 3-*tert*-butyl or 3-isopropyl substituents. Thus, while the exclusive formation of 4-coordinate, pseudotetrahedral $Tp^*M^{II}Cl$ species is most analogous to the chemistry observed for Tp^{tBu} (a so-called "tetrahedral enforcer"), observation of a ~1:1 ratio of η^2:η^3 forms of $Tp^{Menth}Rh(CO)_2$ suggests a decreased steric bulk, more like that of Tp^{iPr_n} (n = 1 or 2). Isolation of an octahedral complex ($Tp^{Menth}TiCl_3$) supports this latter assertion, although its instability with respect to isomerization to $Tp^{Menth*}TiCl_3$ implicates significant steric strain in the C_3-symmetric 6-coordinate structure. Future work will address the efficacy of the highly hindered chiral cavities presented by Tp^{Menth}, Tp^{Menth*}, and $Tp^{Mementh}$ for inducing enantioselective reactivity.

Acknowledgment. We thank Professor Doyle Britton for his work on the X-ray crystal structures and the National Science Foundation (Grant CHE-9207152 and a National Young Investigator Award), the Petroleum Research Fund, administered by the American Chemical Society, and the University of Minnesota Undergraduate Research Opportunities Program (D.D.L.) for financial support. We also thank the reviewers for helpful comments.

Supplementary Material Available: Fully labeled ORTEP drawings and full tables of bond lengths and angles, atomic positional parameters, and final thermal parameters for the X-ray crystal structures of $Tp^{Mementh}ZnCl$, $Tp^{Menth}Ni(OAc)$, and $Tp^{Menth*}TiCl_3{\cdot}CH_2Cl_2$ (31 pages). Ordering information is given on any current masthead page.

(31) Burchill, P.; Wallbridge, M. G. H. *Inorg. Nucl. Chem. Lett.* **1976**, *12*, 93−97.
(32) Hughes, D. L.; Leigh, G. J.; Walker, D. G. *J. Chem. Soc., Dalton Trans.* **1988**, 1153−1157.
(33) Hughes, D. L.; Leigh, G. J.; Walker, D. G. *J. Chem. Soc., Dalton Trans.* **1989**, 1413−1416.
(34) Cano, M.; Heras, J. V.; Jones, C. J.; McCleverty, J. A.; Trofimenko, S. *Polyhedron* **1990**, *9*, 619−621.
(35) Reinaud, O. M.; Rheingold, A. L.; Theopold, K. H. *Inorg. Chem.* **1994**, *33*, 2306−2308.
(36) Rheingold, A. L.; White, C. B.; Trofimenko, S. *Inorg. Chem.* **1993**, *32*, 3471−3477.
(37) Calabrese, J. C.; Trofimenko, S. *Inorg. Chem.* **1992**, *31*, 4810−4814.
(38) Trofimenko, S.; Calabrese, J. C.; Domaille, P. J.; Thompson, J. S. *Inorg. Chem.* **1989**, *28*, 1091−1101.
(39) Looney, A.; Parkin, G. *Polyhedron* **1990**, *9*, 265−276.
(40) The order of stability is opposite for Tp^{Ms} (Ms = mesityl), where the asymmetric Tp^{Ms*} rearranges to the thermodynamically more favored C_{3v}-symmetric Tp^{Ms} at high temperatures.[36]